Enterococcus faecium Biofilm Formation: Identification of Major Autolysin $AtlA_{Efm}$, Associated Acm Surface Localization, and $AtlA_{Efm}$-Independent Extracellular DNA Release

Fernanda L. Paganelli, Rob J. L. Willems, Pamela Jansen, Antoni Hendrickx, Xinglin Zhang, Marc J. M. Bonten, Helen L. Leavis

Department of Medical Microbiology, University Medical Center Utrecht, Utrecht, The Netherlands

ABSTRACT ***Enterococcus faecium*** **is an important multidrug-resistant nosocomial pathogen causing biofilm-mediated infections in patients with medical devices. Insight into *E. faecium* biofilm pathogenesis is pivotal for the development of new strategies to prevent and treat these infections. In several bacteria, a major autolysin is essential for extracellular DNA (eDNA) release in the biofilm matrix, contributing to biofilm attachment and stability. In this study, we identified and functionally characterized the major autolysin of *E. faecium* E1162 by a bioinformatic genome screen followed by insertional gene disruption of six putative autolysin genes. Insertional inactivation of locus tag EfmE1162_2692 resulted in resistance to lysis, reduced eDNA release, deficient cell attachment, decreased biofilm, decreased cell wall hydrolysis, and significant chaining compared to that of the wild type. Therefore, locus tag EfmE1162_2692 was considered the major autolysin in *E. faecium* and renamed $atlA_{Efm}$. In addition, $AtlA_{Efm}$ was implicated in cell surface exposure of Acm, a virulence factor in *E. faecium*, and thereby facilitates binding to collagen types I and IV. This is a novel feature of enterococcal autolysins not described previously. Furthermore, we identified (and localized) autolysin-independent DNA release in *E. faecium* that contributes to cell-cell interactions in the $atlA_{Efm}$ mutant and is important for cell separation. In conclusion, $AtlA_{Efm}$ is the major autolysin in *E. faecium* and contributes to biofilm stability and Acm localization, making $AtlA_{Efm}$ a promising target for treatment of *E. faecium* biofilm-mediated infections.**

IMPORTANCE **Nosocomial infections caused by *Enterococcus faecium* have rapidly increased, and treatment options have become more limited. This is due not only to increasing resistance to antibiotics but also to biofilm-associated infections. DNA is released in biofilm matrix via cell lysis, caused by autolysin, and acts as a matrix stabilizer. In this study, we identified and characterized the major autolysin in *E. faecium*, which we designated $AtlA_{Efm}$. $atlA_{Efm}$ disruption resulted in resistance to lysis, reduced extracellular DNA (eDNA), deficient cell attachment, decreased biofilm, decreased cell wall hydrolysis, and chaining. Furthermore, $AtlA_{Efm}$ is associated with Acm cell surface localization, resulting in less binding to collagen types I and IV in the $atlA_{Efm}$ mutant. We also identified $AtlA_{Efm}$-independent eDNA release that contributes to cell-cell interactions in the $atlA_{Efm}$ mutant. These findings indicate that $AtlA_{Efm}$ is important in biofilm and collagen binding in *E. faecium*, making $AtlA_{Efm}$ a promising target for treatment of *E. faecium* infections.**

Received 1 March 2013 **Accepted** 21 March 2013 **Published** 16 April 2013

Citation Paganelli FL, Willems RJL, Jansen P, Hendrickx A, Zhang X, Bonten MJM, Leavis HL. 2013. *Enterococcus faecium* biofilm formation: identification of major autolysin $AtlA_{Efm}$, associated Acm surface localization, and $AtlA_{Efm}$-independent extracellular DNA release. mBio 4(2):e00154-13. doi:10.1128/mBio.00154-13.

Editor Michael Gilmore, Harvard Medical School

Address correspondence to Helen L. Leavis, h.leavis@umcutrecht.nl.

Enterococci, specifically *Enterococcus faecium* and *Enterococcus faecalis*, are the third most common cause of nosocomial infection (1), and most infections in hospitalized patients are associated with the use of indwelling medical devices, such as (central) venous and urinary catheters (2). A critical step in the pathogenesis of these infections is the colonization of these surfaces by enterococci and the formation of biofilms (3).

The formation of multilayer biofilms involves a complex process, from attachment of single cells to development of a three-dimensional bacterial community, surrounded by an extracellular matrix (4). The matrix is an important component playing a role in biofilm stability and protection against antimicrobials and immune cells (5). It is composed of polysaccharides, proteins, and extracellular DNA (eDNA) (5). eDNA is frequently released in many species by a process called autolysis (6–9) and acts as an adhesive (10), being important for biofilm attachment and stability (6, 8, 11, 12).

In *Pseudomonas aeruginosa*, *Staphylococcus aureus*, *Staphylococcus epidermidis*, and *E. faecalis*, the most important source of eDNA is lysis of a bacterial subpopulation (autolysis), controlled by a quorum-sensing system (6, 13, 14). This process is called fratricide and is mediated by murein hydrolase or autolysin (Atl). Atl has different functions, of which cell separation and autolysis are most important. The repeat domain of Atl can bind to various host extracellular matrix proteins, such as vitronectin, fibrinogen, and fibronectin (15–17).

In the present study, we identified the major autolysin of *E. faecium* and its importance for eDNA release and biofilm formation. Apart from its role in biofilm formation, we demonstrate that $AtlA_{Efm}$ is involved in cell division, morphology, and surface lo-

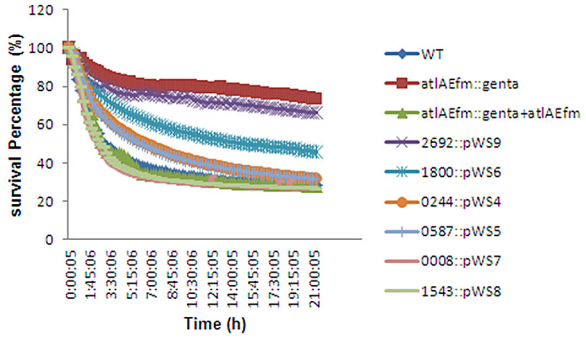

FIG 1 Autolysis induction by Triton X-100 (0.02%). *E. faecium* wild type, predicted autolysin mutants, and the complemented $AtlA_{Efm}$-deficient strain were incubated in the Bioscreen C system at 37°C with continuous shaking, and absorbance at 600 nm (OD_{600}) was recorded every 15 min for 21 h. On the *x* axis, time is indicated in hours (h); on the *y* axis is the percentage of surviving cells in suspension.

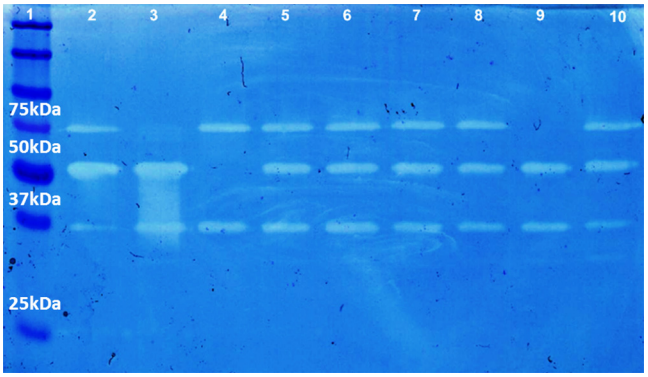

FIG 2 Zymography assay. Hydrolysis of peptidoglycan was analyzed in an SDS-PAGE gel (12%) with crude wild-type cell wall. Lane 1, Precision Plus Protein standards dual color (Bio-Rad); lane 2, wild type; lane 3, 2692::pWS9; lane 4, 1800::pWS6; lane 5, 0244::pWS4; lane 6, 0587::pWS5; lane 7, 0008::pWS7; lane 8, 1543::pWS8; lane 9, $atlA_{Efm}$::genta; lane 10, $atlA_{Efm}$::genta+$atlA_{Efm}$.

calization of Acm, a unique adhesin described in *E. faecium* to bind to collagen types I and IV. Finally, we show the presence of eDNA at the cell septum of the wild-type strain and between the chains of the $AtlA_{Efm}$-deficient mutant. DNase treatment resulted in cell separation, a finding which suggests that eDNA contributes to the chaining phenotype in the $AtlA_{Efm}$-deficient mutant.

RESULTS

Identification of putative *E. faecium* autolysins. Six putative autolysin-encoding genes were selected by bioinformatic analysis, and single-crossover mutants were constructed. Locus tag EfmE1162_2692 has the highest similarity and sequence coverage compared to AtlA in *E. faecalis* (51% amino acid similarity and 80% sequence coverage) (see Table S1 in the supplemental material). Growth curves of these six mutants in brain heart infusion (BHI) broth showed no difference compared to the wild type; however, in tryptic soy broth (TSB) medium with 1% glucose (TSBg), all strains grew to a lower optical density at 600 nm (OD_{600}) than with growth in BHI medium (Fig. S1A and B). Mutant 0587::pWS5 showed earlier log phase in TSBg than did other strains.

The putative autolysin locus tag EfmE1162_2692 is resistant to Triton X-100, exerts peptidoglycan hydrolysis activity, and is involved in cell separation and cell adhesion. Several functional assays were performed to characterize the autolysis activity of the six predicted autolysins. In early stationary phase, bacterial cells are known to be more vulnerable to cell lysis when exposed to Triton X-100 while major autolysin mutants show less lysis (18). Triton X-100 lysis assays of E1162 wild type and the six putative autolysin mutants revealed that with the exception of mutant 2692::pWS9, the OD_{600} of the wild type and the mutants was decreased by 60%. A decrease of only 20% in the OD_{600} was detected in mutant 2692::pWS9, confirming a resistance to lysis (Fig. 1). Therefore, we renamed locus tag EfmE1162_2692 to $atlA_{Efm}$.

Although the observed phenotype of 2692::pWS9 is similar to that of other major autolysins, we attempted to construct a markerless mutant of $atlA_{Efm}$ (see Materials and Methods), but unfortunately, this was unsuccessful. As an alternative, we selected from a mariner transposon library in E1162 a mutant ($atlA_{Efm}$::genta) that contained an insertion of a gentamicin resistance gene at position 278 relative to the start of the gene. This insertion of a single resistance gene is considerably smaller than pWS9 and even less likely to result in polar effects on adjacent genes that encode a type 2 phosphatidic acid phosphatase family protein (upstream) and a leucyl-tRNA synthetase (downstream). However, to confirm that all observed phenotypes were attributed only to insertional inactivation of $atlA_{Efm}$, we complemented $atlA_{Efm}$::genta in *trans*, resulting in $atlA_{Efm}$::genta+$atlA_{Efm}$.

Growth curves of $atlA_{Efm}$::genta in BHI medium showed no difference compared to the wild type, while in TSBg, $atlA_{Efm}$::genta reached a higher OD in stationary phase (see Fig. S1A and B in the supplemental material). As shown in $atlA_{Efm}$::pWS9, $atlA_{Efm}$::genta is also resistant to lysis when analyzed in the Triton X-100 assay (Fig. 1).

$AtlA_{Efm}$ contains six LysM domains which are conserved in other major autolysins and have been shown to be able to bind and hydrolyze peptidoglycan from the cell wall, causing cell death (19). To confirm hydrolysis of peptidoglycan by $AtlA_{Efm}$, supernatants of the wild type, all predicted autolysin mutants, and the complemented strain $atlA_{Efm}$::genta+$atlA_{Efm}$ were subjected to zymography. In Fig. 2, three autolytic bands of 75, 50, and 37 kDa were observed. Mutants 2692::pWS9 and $atlA_{Efm}$::genta lacked the 75-kDa band compared to the wild type and the complemented strain, a band which is the expected size of the major autolysin $AtlA_{Efm}$. The second band of approximately 50 kDa was missing from the mutant 1800::pWS6. Fifty kilodaltons is the expected size of locus tag EfmE1162_1800 (46.8 kDa), indicating that this gene possibly encodes a secondary autolysin. None of the screened mutants lacked the third autolytic band (37 kDa).

By hydrolyzing peptidoglycan, autolysins can play a role in cell separation and growth. Chaining of bacterial cells, a result of impaired cell partitioning, has been observed in other species when the major autolysin gene is inactivated. In overnight cultures, long chains of $atlA_{Efm}$::genta were observed, implying the cell separation defect (see Fig. S2A to H in the supplemental material). No chaining was observed in the other predicted autolysin mutants or in the complemented $atlA_{Efm}$ mutant.

Since in other bacterial species, autolysins are also implicated in early attachment of cells, we subsequently studied early adhesion on polystyrene of the wild type and the six putative autolysin mutants. Only $atlA_{Efm}$::genta had substantially fewer cells attached

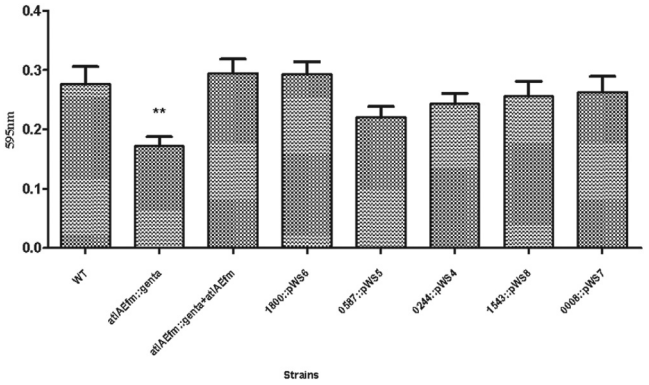

FIG 3 Adhesion assay. The wild type, predicted autolysin mutants, and the complemented $AtlA_{Efm}$-deficient strain at an OD_{660} of 0.3 were incubated for 2 h at 37°C without shaking in a 96-well plate. Cell attachment was measured by absorbance of crystal violet at 595 nm.

(33%) than the wild type (Fig. 3), while attachment was restored in the complemented strain *atlA*$_{Efm}$::genta+*atlA*$_{Efm}$.

In conclusion, *atlA*$_{Efm}$::genta not only was less vulnerable to Triton X-100 and less capable of initial adherence but also reduced peptidoglycan hydrolysis activity and exhibited long chaining, supporting that this gene serves as the actual major autolysin in *E. faecium*.

$AtlA_{Efm}$ is a prerequisite for normal biofilm development in *E. faecium*. We studied the effect of autolysin mutants on biofilm formation in three different models: polystyrene, semistatic, and flow cell models. In the polystyrene model, all predicted autolysin mutants were tested, and only *atlA*$_{Efm}$::genta formed 80% less biofilm than the wild type while biofilm formation was restored in the complemented mutant (see Fig. S3 in the supplemental material).

Due to this result, only *atlA*$_{Efm}$::genta was tested in the other assays. In the semistatic model, biofilm formation of *atlA*$_{Efm}$::genta was considerably reduced compared to that of the wild type. Average thickness was reduced by 80% while biomass was reduced by 90% relative to that of the wild type. This phenotype was complemented in *atlA*$_{Efm}$::genta+*atlA*$_{Efm}$ (Fig. 4A to C).

In a flow cell model, biofilm formation of the $AtlA_{Efm}$ mutant was also attenuated. In this model, wild-type cells firmly attached to the slide, formed small clumps, and developed into thick biofilm covering the whole slide within a few hours. In contrast, *atlA*$_{Efm}$::genta was impaired in initial attachment and subsequently formed only small and thin clumps, which were not stable enough to develop to mature biofilm at 17 h of growth (see Movie S1A in the supplemental material). Again, the wild-type

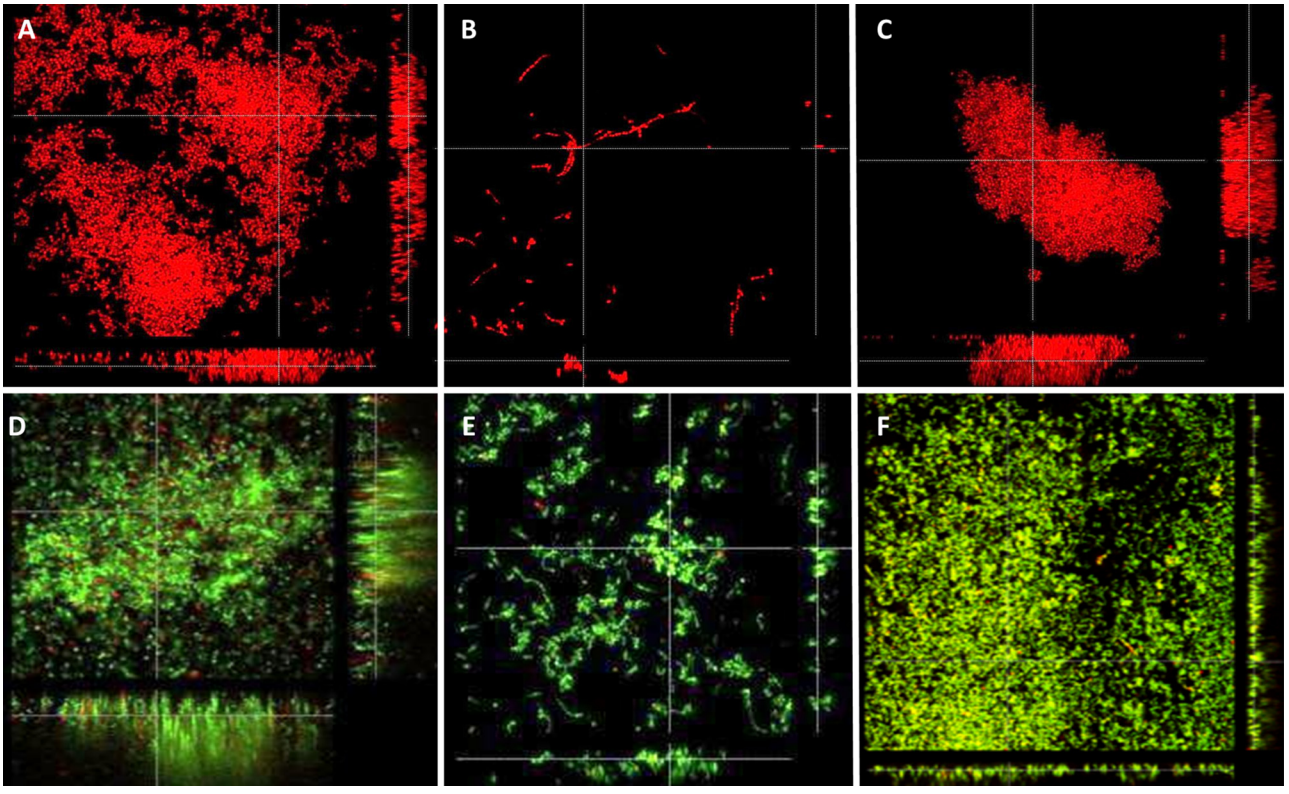

FIG 4 Confocal microscopy images of the semistatic biofilm model and the flow cell biofilm model. Biofilm of the wild type (A), *atlA*$_{Efm}$::genta (B), and *atlA*$_{Efm}$::genta+*atlA*$_{Efm}$ (C) was grown for 24 h on poly-L-lysine-coated glass in TSBg at 120 rpm at 37°C. Cells were stained with propidium iodide (red). The average thickness and biomass of biofilms were measured at five random positions and analyzed with Comstat/Matlab software. The average thickness was 1.86 μm for the wild type, 0.14 μm for *atlA*$_{Efm}$::genta, and 0.84 μm for *atlA*$_{Efm}$::genta+*atlA*$_{Efm}$. The mean biomass was 0.73 $\mu m^3/\mu m^2$ for the wild type, 0.03 $\mu m^3/\mu m^2$ for *atlA*$_{Efm}$::genta, and 0.45 $\mu m^3/\mu m^2$ for *atlA*$_{Efm}$::genta+*atlA*$_{Efm}$. The difference between the wild type and the mutant was significant ($P < 0.005$). Pictures were taken at ×63 magnification with a 2.5 optical zoom. In the flow cell model, biofilm was grown for 17 h in a Stovall flow cell system in 1:10 TSB with 1% glucose (0.13 ml/min) at 37°C. Pictures were taken at ×40 magnification with a 2.5 optical zoom for the wild type (D), a 3.5 optical zoom for *atlA*$_{Efm}$::genta (E), and a 2.5 optical zoom for *atlA*$_{Efm}$::genta+*atlA*$_{Efm}$ (F). Cells were stained with Syto 9 (green) and propidium iodide (red).

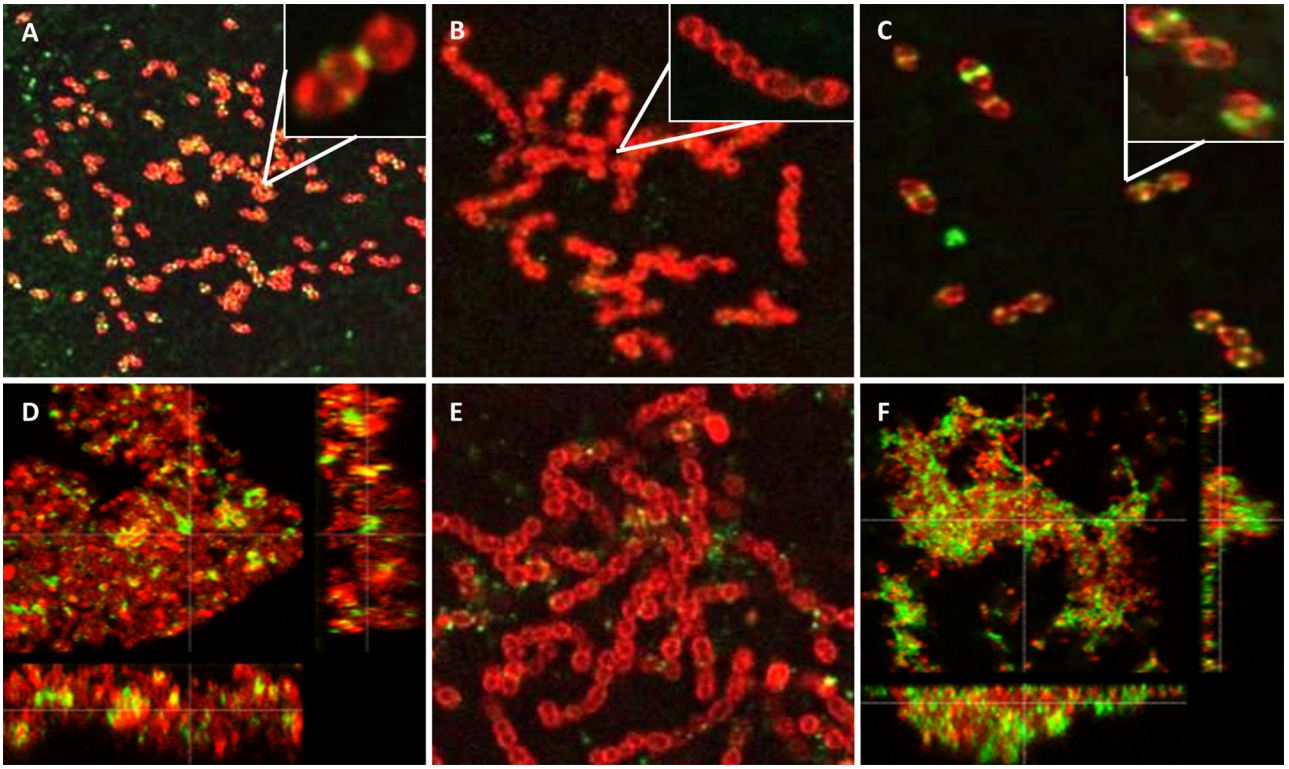

FIG 5 Confocal microscopy close-up images of surface-localized $AtlA_{Efm}$ in planktonic cells and biofilm. Pictures were taken at ×63 magnification with 4.2 and 41.9 optical zooms for the wild type (A), 5.8 and 15.0 optical zooms for *atlA*$_{Efm}$::genta (B), and 7.3 and 31.6 optical zooms for *atlA*$_{Efm}$::genta+*atlA*$_{Efm}$ (C) at an OD_{660} of 0.3 of planktonic cells. For the biofilm model, pictures were taken at ×63 magnification with a 5.1 optical zoom for the wild type (D), a 9.7 optical zoom for *atlA*$_{Efm}$::genta (E), and a 3.7 optical zoom for *atlA*$_{Efm}$::genta+*atlA*$_{Efm}$ (F). Cells were incubated with α-$AtlA_{Efm}$ and goat α-rabbit Alexa 488 (green). The bacterial membrane was stained with FM 95-5 (red).

phenotype was restored when the mutant was complemented (Fig. 4D to F).

$AtlA_{Efm}$ is cell surface localized at the septum and is secreted in biofilm. In other bacterial species, the major autolysin has been identified both in the supernatant of planktonic cells and localized to the bacterial surface (11, 20). We used $AtlA_{Efm}$-specific antibodies to detect cell surface expression of $AtlA_{Efm}$ in planktonic cells. Flow cytometry analysis demonstrated that $AtlA_{Efm}$ was detected at the wild-type cell surface, with higher expression in log phase than stationary phase (data not shown). $AtlA_{Efm}$ antibodies were specific, since in all of the following experiments, incubations with secondary antibodies alone yielded no signal.

In addition, confocal microscopy showed that $AtlA_{Efm}$ was also localized at the septum of cells in log phase, supporting a role in cell separation, as already concluded from the chaining phenotype in the mutant (Fig. 5A). As expected, no $AtlA_{Efm}$ signal was observed from the mutant (Fig. 5B). In the complemented strain (Fig. 5C), the same septum localization as that identified in the wild type was observed. In 24-h biofilms, $AtlA_{Efm}$ was not specifically localized at the septum of the cells but was identified between cells in the matrix and randomly around a subset of cells. In the mutant, again, no $AtlA_{Efm}$ was detected, while the complemented strain exhibited the same localization of $AtlA_{Efm}$ as the wild type (Fig. 5D to F).

$AtlA_{Efm}$ contributes to eDNA release and eDNA-dependent biofilm formation. By exerting lysis activity, autolysins can contribute to eDNA release in planktonic cells and also in biofilm, thereby contributing to biofilm formation and stability. The presence of eDNA in *E. faecium* wild type, *atlA*$_{Efm}$::genta, and *atlA*$_{Efm}$::genta+*atlA*$_{Efm}$ was analyzed by isolation of DNA present in the supernatant of overnight cultures. As shown in Fig. S4 in the supplemental material, supernatant of *atlA*$_{Efm}$::genta contained less DNA than the wild type and the complemented strain. To further investigate the role of eDNA in biofilm, we studied the effect of DNase in a semistatic biofilm model. Incubation with DNase at a *t* of 0 reduced biofilm biomass and average biofilm thickness by 94% and 91%, respectively, in the wild type and *atlA*$_{Efm}$::genta+*atlA*$_{Efm}$ after 24 h of biofilm growth (Fig. 6A, B, E, and F). These results show that eDNA is important in biofilm formation. Unexpectedly, incubation of the mutant with DNase leads to separation of bacterial chains into single cells and increased cell attachment but not clump and biofilm formation (Fig. 6C and D). Similar to the biofilm semistatic model, chains were separated within 5 min during planktonic growth in an eight-well chamber slide when DNase was added to *atlA*$_{Efm}$::genta (Movie S1B).

To further investigate how DNase treatment results in chain separation, we incubated 4-h and 24-h biofilms and overnight-cultured planktonic cells with double-stranded DNA (dsDNA) antibodies. Using confocal microscopy, we were able to detect DNA at the cell septum in wild-type 4-h early biofilm (Fig. 7A and B) and between the chains of overnight planktonic growth of *atlA*$_{Efm}$::genta (Fig. 7C and D), results which concur with our observations of the effect of DNase on cell separation in the chained *atlA*$_{Efm}$::genta and suggest that eDNA contributes to the chaining

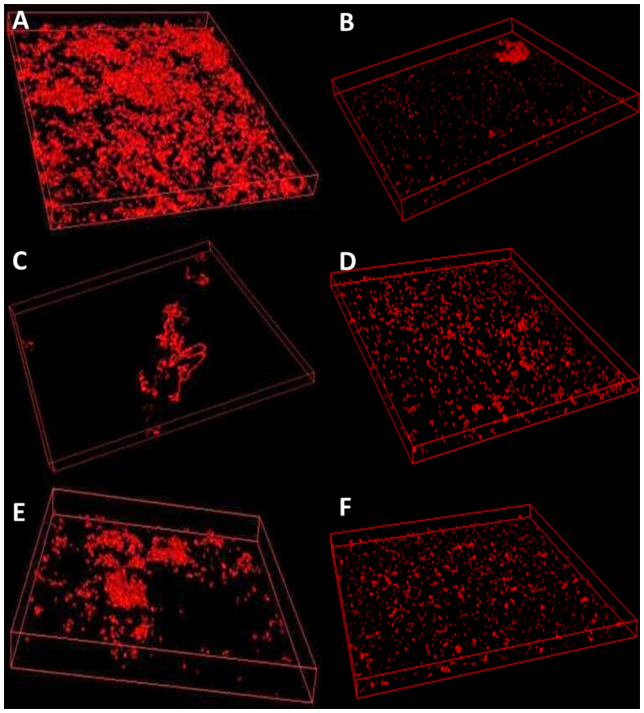

FIG 6 Effect of DNase in biofilm formation. Confocal images of wild-type biofilm, cultured without (A) and with (B) DNase, *atlA*$_{Efm}$::genta biofilm cultured without (C) and with (D) DNase, and *atlA*$_{Efm}$::genta+*atlA*$_{Efm}$ biofilm cultured without (E) and with (F) DNase. Twenty-four-hour biofilm was grown in a semistatic model in TSBg at 120 rpm at 37°C. Cells were stained with propidium iodide. When DNase was added, the average thickness was 0.068 μm for the wild type, 0.099 μm for *atlA*$_{Efm}$::genta, and 0.10 μm for *atlA*$_{Efm}$::genta+*atlA*$_{Efm}$. The mean biomass was 0.019 $\mu m^3/\mu m^2$ for the wild type, 0.037 $\mu m^3/\mu m^2$ for *atlA*$_{Efm}$::genta, and 0.035 $\mu m^3/\mu m^2$ for *atlA*$_{Efm}$::genta+*atlA*$_{Efm}$. The difference between biofilms with and without DNase was significant for the wild type and the complemented AtlA$_{Efm}$-deficient strain ($P < 0.05$). Pictures were taken at ×63 magnification with a 2.5 optical zoom.

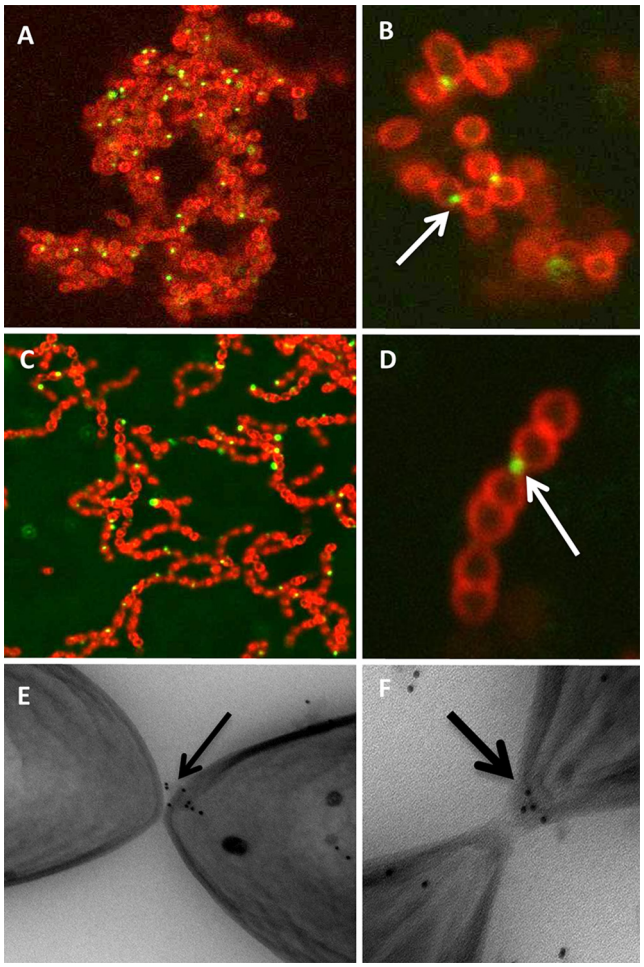

FIG 7 Confocal microscopy and transmission electron microscopy close-up images of eDNA. Pictures were taken at ×63 magnification with 6.6 and 15.5 optical zooms for wild-type 4-h biofilm (A and B) and 6.5 and 27.0 optical zooms for overnight-cultured *atlA*$_{Efm}$::genta (C and D). Cells were incubated with α-dsDNA and goat α-mouse Alexa 488 (green). The bacterial membrane was stained with FM 95-5 (red). Transmission electron microscopy of *atlA*$_{Efm}$::genta overnight cultures (E and F). Cells were incubated with α-dsDNA and rabbit α-mouse of the same isotype. Immunogold particles are seen linked to wire-like structures between the cells as well as to polymeric structures outside cells, which likely represents released DNA.

phenotype in the AtlA$_{Efm}$-deficient mutant. Immunoelectron microscopy clearly showed the chaining phenotype in the AtlA$_{Efm}$-deficient mutant, confirmed by α-dsDNA gold incubation labeling of eDNA at the cell septum of *atlA*$_{Efm}$::genta chains from overnight cultures (Fig. 7E and F). In both methods, incubation with only secondary antibodies of the same isotype did not give specific signals (see Fig. S5E and F in the supplemental material). In 4-h and 24-h *atlA*$_{Efm}$::genta biofilms, DNA was also observed between the cells (Fig. S5B and C).

The effect of exogenous AtlA$_{Efm}$ on phenotypes of wild-type and mutant strains was studied using confocal microscopy. For this, the wild type, *atlA*$_{Efm}$::genta, and *atlA*$_{Efm}$::genta+*atlA*$_{Efm}$ were incubated with or without AtlA$_{Efm}$ in BHI in an eight-well chamber. When AtlA$_{Efm}$ was added, as with DNase, chains started to be released into separate cells in the AtlA$_{Efm}$-deficient mutant, but unlike DNase, clumping of cells occurred in all strains. It is important to mention that this phenomenon was observed in BHI, a medium in which *E. faecium* forms less-established biofilms (see Movie S1C in the supplemental material).

These results indicate that AtlA$_{Efm}$ plays different roles in biofilm, where it contributes to biofilm stability via eDNA release, and during planktonic growth, where it may induce cell clumping.

AtlA$_{Efm}$ influences surface protein localization and binding to collagen types I and IV. Some autolysins are known to act as adhesins and may bind extracellular matrix (ECM) proteins (microbial surface components recognizing adhesive matrix molecules [MSCRAMMs]). Therefore, we verified the role of AtlA$_{Efm}$ in binding to ECM proteins using a whole-cell enzyme-linked immunosorbent assay (ELISA). When the wild type, *atlA*$_{Efm}$::genta, and *atlA*$_{Efm}$::genta+*atlA*$_{Efm}$ were incubated with ECM proteins, the AtlA$_{Efm}$-deficient mutant, unlike the wild type and the complemented strain, specifically did not bind to collagen types I and IV (Fig. 8). To confirm whether AtlA$_{Efm}$ is responsible for this phenotype, an ELISA with the purified protein was conducted; however, no binding of purified AtlA$_{Efm}$ to collagen types I and IV was observed (data not shown).

Since AtlA$_{Efm}$ seemed not directly involved in collagen binding, we hypothesized that AtlA$_{Efm}$ contributed to cell surface expression of another collagen-binding surface protein. Nallapareddy et al. (21) described Acm, a collagen-binding adhesin,

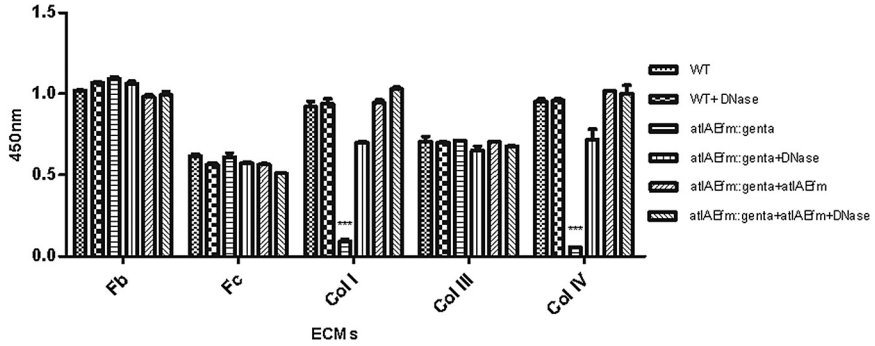

FIG 8 Adherence of planktonic cells to ECM proteins by whole-cell ELISA. Binding of the wild type, $atlA_{Efm}$::genta, and $atlA_{Efm}$::genta+$atlA_{Efm}$ to fibrinogen (Fb), fibronectin (Fc), collagen type I (Col I), collagen type III (Col III), and collagen type IV (Col IV) was detected using α-enterococcus serum followed by goat α-rabbit IgG horseradish peroxidase (HRP) antibodies.

which, so far, is the only *E. faecium* surface protein that specifically binds to collagen types I and IV.

Confocal microscopy using α-Acm antibodies revealed that Acm was localized at the septum and at the poles in the wild type and the complemented strain, while in $atlA_{Efm}$::genta, Acm was localized only at the septum (Fig. 9A to C). Control antibodies from the same isotype gave no labeling (see Fig. S6B in the supplemental material). Absence of exposed Acm at the poles of the $AtlA_{Efm}$-deficient mutant most probably resulted from the defect in cell separation in this strain and may explain the reduced binding to collagen types I and IV. Specificity of α-Acm antibodies was confirmed, since flow cytometry revealed, unlike with the E1162 wild type, no Acm expression in strain E980, a commensal isolated with a transposon insertion in *acm* (Fig. S6A).

To confirm the later hypothesis, the $AtlA_{Efm}$-deficient mutant was tested for collagen type I and IV binding in a whole-cell ELISA in the presence of DNase, which, as demonstrated above, resolves the long chains in this mutant. As expected, incubation of the $atlA_{Efm}$::genta mutant with DNase restored binding to collagen types I and IV (Fig. 8).

DISCUSSION

In this study, we identified and characterized the major autolysin in *E. faecium*, $AtlA_{Efm}$, and demonstrated that $AtlA_{Efm}$, as in other species, is directly involved in biofilm formation, cell separation, cell wall hydrolysis, and eDNA release (22). Furthermore, the $AtlA_{Efm}$-deficient mutant displayed attenuated cell surface localization of Acm.

Based on sequence similarity, $AtlA_{Efm}$ is composed of three domains, a central catalytic domain, responsible for glucosaminidase activity (23), a C-terminal domain, composed of LysM modules that afford peptidoglycan affinity and possibly target autolysins to the division septum and poles (24), and a T/E-rich N-terminal domain, the function of which is still unknown (23). Like the major autolysin of *E. faecalis* (14), $AtlA_{Efm}$ contains a lysozyme-like superfamily domain and six LysM domains which are not present in any of the other putative autolysins analyzed. Lysozyme-like superfamily domains are known to be involved in the hydrolysis of beta-1,4-linked polysaccharides (25). Moreover, $atlA_{Efm}$ is present in all sequenced *E. faecium* strains, suggesting a highly conserved and essential function.

Five types of experiments indicated that $AtlA_{Efm}$ is the major autolysin of *E. faecium*. First, the $AtlA_{Efm}$-deficient mutant demonstrated considerably less cell lysis in the presence of Triton X-100 than did the wild type. Second, in the zymography, a lytic band of 75 kDa, which is identical to the predicted molecular mass of $AtlA_{Efm}$, was identified as $AtlA_{Efm}$. Third, the $AtlA_{Efm}$-deficient mutant showed decreased early adhesion compared to that of the wild type. Fourth, devious cell separation by chain formation was observed only in the $AtlA_{Efm}$-deficient mutant, and finally, the $AtlA_{Efm}$-deficient mutant had 80% less biofilm production than the wild type in a polystyrene assay. All phenotypes were able to be restored by complementation in *trans*. These five lines of evidence demonstrate that $AtlA_{Efm}$ plays a major role in *E. faecium* E1162 autolysis and should be considered the major autolysin. In addition to $AtlA_{Efm}$, we identified a second autolysin (locus tag EfmE1162_1800) by zymography. In *E. faecalis*, a second autolysin, designated AtlB, has lytic properties and can act as a surrogate of AtlA but is less efficient in cell separation, probably due to the presence of fewer LysM domains (26). Also in *E. faecium*, locus tag EfmE1162_1800 has only two LysM domains, compared to the six domains in $AtlA_{Efm}$. The exact function of this second autolysin remains to be investigated.

Confocal microscopic observations revealed that the $AtlA_{Efm}$-deficient mutant formed long chains of cells compared to the wild type in planktonic growth and biofilm. The formation of long chains of cells upon inactivation of the major autolysin has also been observed previously (27, 28) and implies that autolysin plays a role in cell separation. Our findings that $AtlA_{Efm}$ was localized at the septum of cells in log phase and that addition of exogenous $AtlA_{Efm}$ resolved chained cells into single cells support a role of $AtlA_{Efm}$ in cell separation. Schlag et al. (19) elucidated the mechanism underpinning localized peptidoglycan hydrolysis in staphylococci. Although wall teichoic acid prevents *S. aureus* Atl from binding to the cell wall, binding of Atl through its amidase domain at the cell septum is increased, presumably due to a lower wall teichoic acid concentration (19). This mechanism explains why autolysin-derived peptidoglycan hydrolases are active primarily at the site of cell separation (29, 30). In *E. faecalis*, cell chaining in an AtlA mutant disappeared after 24 h of culture, indicating that eventually AtlB can cleave the cell septum in the absence of AtlA (31). However, this does not apply to *E. faecium*, since chaining was also observed in overnight-cultured $atlA_{Efm}$::genta and in all other conditions tested.

An unexpected finding was that addition of DNase to the $AtlA_{Efm}$-deficient mutant also resulted in chains resolving into

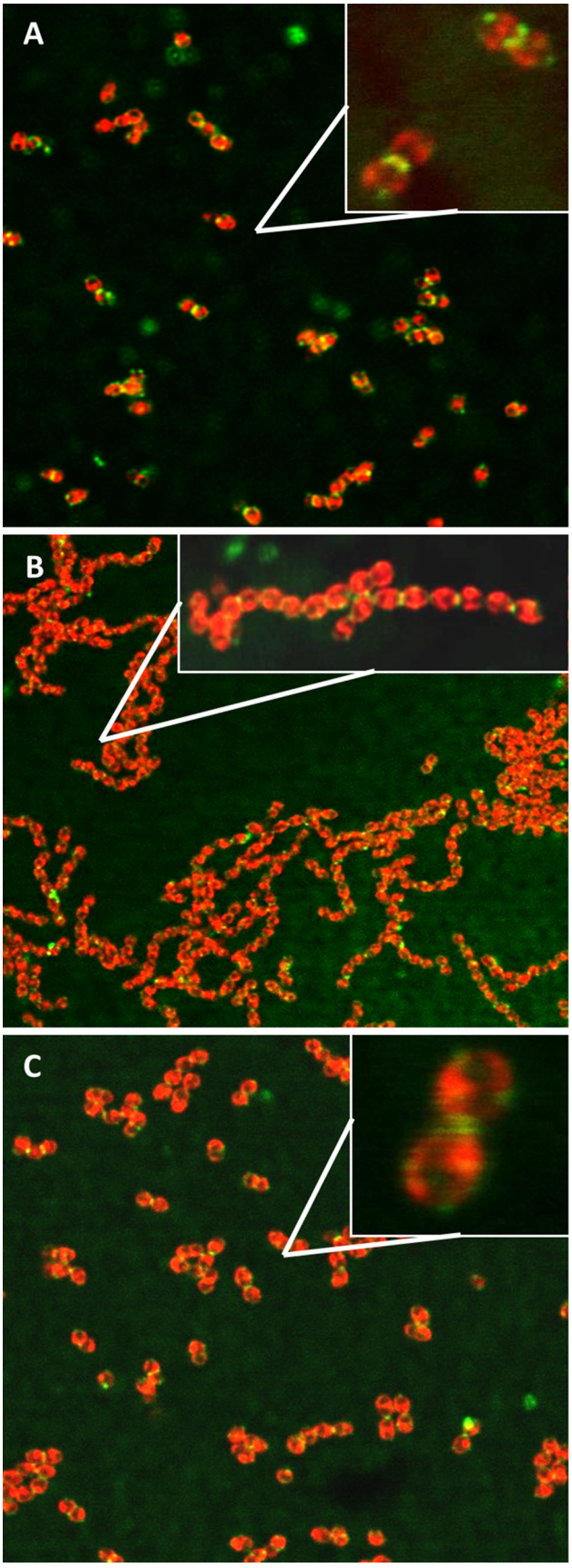

single cells. This means that for the first time we have demonstrated that DNA plays a role in cell-cell interactions in *E. faecium*. In *E. faecalis*, DNA can be secreted by metabolically active cells in the absence of lysis, and this actively secreted eDNA is present at the cell septum and important in early biofilm formation (32). As in *E. faecalis*, we were able to demonstrate that in wild-type *E. faecium* and in the $AtlA_{Efm}$-deficient mutant, eDNA is present at the cell septum. Specifically, the fact that this was also seen in the $AtlA_{Efm}$-deficient mutant supports the hypothesis that also in *E. faecium*, eDNA was able to be released in the absence of a major autolysin and is involved in cell separation. Together, these results indicate that both peptidoglycan and eDNA are involved in cell-cell interactions upon cell division that allow both $AtlA_{Efm}$ and DNase to separate the bacterial chains. The exact organization of peptidoglycan and eDNA at the cell septum and the possible interaction between these two components are currently not known and remain to be elucidated.

We also demonstrated the presence of $AtlA_{Efm}$ in the biofilm matrix. As in *E. faecalis*, $AtlA_{Efm}$ might be involved in autolysis of a subpopulation in the biofilm by a fratricidal mechanism (14). In *E. faecalis*, this is mediated by the protease GelE and coordinated by a two-component system. Such a regulatory mechanism of $AtlA_{Efm}$ expression is currently unknown in *E. faecium*.

Incubation of a single layer of $AtlA_{Efm}$-deficient mutant cells with purified $AtlA_{Efm}$ resulted in clump formation, suggesting that secretion of $AtlA_{Efm}$ contributes to this process. This indicates that $AtlA_{Efm}$ may have different functions during planktonic and biofilm lifestyles of *E. faecium*.

Biofilm formation is a multistep process that requires bacterial adhesion to a substrate followed by cell-cell interactions, resulting in multiple layers of biofilm. Apart from impaired initial adherence of the $AtlA_{Efm}$-deficient mutant, which may be attributed to the chaining phenotype (33–35), the biofilm deficiency also seemed to result from reduced stability of the matrix in biofilm clumps. This is most probably due to reduced amounts of eDNA but might also be due to a lack of cohesive activity of $AtlA_{Efm}$ when secreted in biofilm.

Apart from biofilm formation, cell attachment through binding to ECM proteins is an important step in colonization. We observed reduced binding of the $AtlA_{Efm}$-deficient mutant to collagen types I and IV, most likely due to altered localization of Acm. Peptidoglycan hydrolases, in general, have been described to be involved in surface protein assembly, specifically proteins related to secretion systems in Gram-negative bacteria (36). However, this is the first documentation of the role of a major autolysin in protein surface localization in Gram-positive bacteria. This observation implies an essential contribution of $AtlA_{Efm}$ to *E. faecium* colonization, since Acm seems to be the major collagen-binding surface protein. Collagen type I is the most common collagen in the human body and is found in all tissues, while collagen type IV is present exclusively in the basal lamina (37), for instance in the gut, which is an important niche of *E. faecium*.

FIG 9 Confocal microscopy images of surface-localized Acm in planktonic cells. Pictures were taken at ×63 magnification with 5.9 and 29.5 optical zooms for the wild type (A), 4.6 and 12.0 optical zooms for $atlA_{Efm}$::genta (B), and 6.5 and 39.1 optical zooms for $atlA_{Efm}$::genta+$atlA_{Efm}$ (C). Planktonic cells were cultured in BHI broth until stationary phase at 37°C. Cells were incubated with α-Acm and goat α-rabbit Alexa 488 (green). The bacterial membrane was stained with FM95-5 (red).

The results presented here provide insights into how $AtlA_{Efm}$, a newly identified major autolysin in *E. faecium*, plays an important role in cell lysis and separation, biofilm formation, cell adhesion, and Acm localization and thus may contribute to the pathogenesis of *E. faecium* infections. Expression, distribution, and activation of the autolysin are probably tightly controlled in *E. faecium*, and these mechanisms need to be elucidated.

Nosocomial *E. faecium* infections are caused by multiresistant strains, which tend to even become panresistant. In addition, current drugs fail to eradicate biofilms and new drugs are barely needed. Although animal models did not show a reduction in virulence of AtlA-deficient mutants in *E. faecalis* (38), we expect $AtlA_{Efm}$ to behave differently. First, genetic inactivation of the major autolysin $AtlA_{Efm}$ affects not only biofilm formation but also binding to the ECM collagen types I and IV. Second, after prolonged growth, no apparent replacement of $AtlA_{Efm}$ function by the secondary autolysin, as in *E. faecalis*, occurs. Therefore, $AtlA_{Efm}$ may serve as a promising candidate for development of new targeted strategies in the treatment of *E. faecium* biofilm-related infections (39).

MATERIALS AND METHODS

Identification of putative *E. faecium* autolysins. A bioinformatic screen was performed to identify putative autolysins in the *E. faecium* E1162 genome (40). Using BLASTp (http://www.ncbi.nlm.nih.gov/), six genes were selected for further characterization based on amino acid similarity to *atlA* from *E. faecalis* V583 (see Table S1 in the supplemental material).

Bacterial strains, plasmids, growth conditions, and determination of growth curves. *E. faecium* and *Escherichia coli* strains used in this study are listed in Table S2 in the supplemental material. The ampicillin-resistant *E. faecium* strain E1162, recently sequenced in our lab, was used throughout this study (40). Unless otherwise mentioned, *E. faecium* was grown in BHI at 37°C. For biofilm assays, TSBg was used. *E. coli* DH5α, BL21 (Invitrogen), and EC1000 (41) were grown in Luria-Bertani (LB) medium. Where necessary, antibiotics (Sigma-Aldrich, Saint Louis, MO) were used at the following concentrations: gentamicin, 300 μg/ml (*E. faecium*) and 25 μg/ml (*E. coli*); spectinomycin, 300 μg/ml (*E. faecium*) and 100 μg/ml (*E. coli*); erythromycin, 50 μg/ml with added lincomycin at 50 μg/ml (*E. faecium*) and 150 μg/ml (*E. coli*); and ampicillin, 150 μg/ml (*E. coli*). Determination of growth curves in triplicate was described by Zhang et al. (42) using a Bioscreen C instrument (Oy Growth Curves AB).

Gene disruption and mutant complementation. Predicted autolysin genes were disrupted and complemented as described before (43). Gene-specific primers and modified pWS3 vectors are mentioned in Table S3 in the supplemental material, resulting in single-crossover mutant strains in Table S2. To confirm the phenotype of 2692::pWS9, we tried to construct a markerless mutant using the approach previously described by us (42); however, complete or partial markerless deletion of $atlA_{Efm}$ was unsuccessful. Therefore, we screened 400 clones from a mariner transposon mutant library for reduced biofilm formation in polystyrene plates and selected a mutant that carried the gentamicin resistance gene *aac(6′)-aph(2″)* as an insertion in $atlA_{Efm}$, $atlA_{Efm}$::genta (42). Finally, $atlA_{Efm}$::genta was complemented using a modified pMSP3535 vector (44) (Table S2). For that, the entire $atlA_{Efm}$ gene was amplified using primers $atlA_{Efm}$-comp-BamHI-F and $atlA_{Efm}$-comp-XhoI-R (Table S3) and cloned in pMSP3535, resulting in pMSP3536. pMSP3536 was introduced in $atlA_{Efm}$::genta by electroporation, resulting in $atlA_{Efm}$::genta+$atlA_{Efm}$.

Autolysis assay. To monitor bacterial lysis, overnight cultures of wild-type *E. faecium*, all single-crossover mutants, $atlA_{Efm}$::genta, and the in *trans*-complemented strain $atlA_{Efm}$::genta+$atlA_{Efm}$ were inoculated at an initial OD_{660} of 0.05 into 5 ml BHI and incubated at 37°C. Cells at an OD_{660} of 0.5 were washed with phosphate-buffered saline (PBS) and resuspended in 0.02% Triton X-100. Cell suspensions were incubated in the Bioscreen C system at 37°C with continuous shaking, and absorbance at 600 nm was recorded every 15 min for 21 h. Each experiment was performed in triplicate.

Zymography. A zymographic analysis of cell wall-associated hydrolases was conducted as described by Liu et al. (45) and Ju et al. (46) with some modifications. Briefly, extracellular murein hydrolases of the wild type, all mutants, and the complemented strain $atlA_{Efm}$::genta+$atlA_{Efm}$ were collected from 50 ml BHI medium at an OD_{660} of 0.3. To prepare substrates for the zymogram, 300 ml of wild-type overnight BHI culture was used to extract the cell wall from the bacteria. Lytic activity as a result of cell wall hydrolysis appeared as a white band on a blue background.

Initial polystyrene adherence assay. The initial adherence assay was performed in triplicate as described previously with minor modifications (47). *E. faecium* strains cultured overnight in BHI were diluted up to an OD_{660} of 0.05 and grown until an OD_{660} of 0.3. Two-hundred-microliter bacterial suspensions were added in triplicate to the polystyrene plate. Bacteria were stained with crystal violet and eluted with 96% ethanol.

Biofilm polystyrene assay. The biofilm polystyrene assay was performed in triplicate as described previously with some modifications (47). In brief, plate-grown bacteria were resuspended in TSBg and the OD_{660} was measured. Cell suspensions were diluted to an OD_{660} of 0.01 and incubated for 24 h. The plates were washed and stained as described above.

Biofilm semistatic model and CLSM. For the biofilm semistatic model, overnight bacterial cultures were diluted to an OD_{660} of 0.01 in 6 ml TSBg and added to a coverslip coated with poly-L-lysine (0.45 μm; diameter, 12 mm; Becton Dickinson) inside a well from a six-well polystyrene plate (Corning Inc.). When applied, 1.5 μg/μl of DNase (Roche) was added at the start of the biofilm ($t = 0$). Biofilms were grown at 37°C for 24 h at 120 rpm. After 24 h, the coverslips were washed once with 0.85% NaCl, and the biofilms were chemically fixed in 8% glutaraldehyde (Merck) for 20 min and washed again with 0.85% NaCl. The biofilms were stained with 15 μg/ml propidium iodide (PI) in 0.85% NaCl for 15 min. After incubation, the stain was removed and coverslips were transferred to glass microscope slides and analyzed by a confocal laser scanning microscope (CLSM) (Leica SP5), equipped with an oil plan-Neofluar ×63/1.4 objective. PI was excited at 633 nm. Z stacks were taken with an interval of 0.42 μm. Pictures were analyzed with LAS AF software (Leica), and biofilm was quantified using Comstat (48)/Matlab R2010b software (the MathWorks). The average thickness and biomass of the biofilms were measured at five randomly chosen positions.

Flow cell biofilm model. Dynamic biofilms were studied in a Stovall flow cell system (Life Science, Inc., Greensboro, NC). Twenty-four-hour TSB cultures were diluted until an OD_{660} of 0.01 and inoculated in the chambers. Biofilms were grown in TSB diluted in PBS (1:10 [vol/vol]) with 1% glucose under a flow of 0.13 ml/min during 17 h. Biofilm development was scanned at regular intervals of 7 min (×40 objective) with a DFC360 FX digital camera kit SP5 (Leica). After 17 h, the flow was increased to 0.5 ml/min to wash away loose cells. Final biofilms were stained with live/dead stain (BAC light kit; Invitrogen), and images were acquired using a confocal microscope (Leica SP5).

eDNA isolation. Total eDNA from the E1162 wild type, $atlA_{Efm}$::genta, and $atlA_{Efm}$::genta+$atlA_{Efm}$ was isolated from BHI overnight cultures with isopropanol and ethanol precipitation as described previously (14).

Cloning, expression, and purification of recombinant $AtlA_{Efm}$. The E1162 $atlA_{Efm}$ gene was amplified with $atlA_{Efm}$-exp-BamHI-F and $atlA_{Efm}$-exp-NotI-R primers (see Table S3 in the supplemental material) and cloned in frame into the expression plasmid (Table S2), expressed and purified as previously described by Bardoel et al. (49).

α-$AtlA_{Efm}$ and α-Acm polyclonal rabbit antisera. Highly specific polyclonal rabbit antisera were prepared by Eurogentec (Seraing, Belgium) according to their classic 28-day anti-protein polyclonal antibody protocol (https://secure.eurogentec.com/products/custom-polyclonal-antibodies.html). Two specific-pathogen-free rabbits were immunized with 200 μg purified $AtlA_{Efm}$. For eliciting Acm polyclonal antisera,

rabbits were immunized with a synthetic peptide (KLH-WEPVPDAETKRLDNGC) based on the amino acid sequence (locus tag EfmE1162_1704) according to the 28-day anti-peptide protocol of Eurogentec.

Flow cytometry. $AtlA_{Efm}$ and Acm were detected at the surface of *E. faecium* E1162, $atlA_{Efm}$::genta, $atlA_{Efm}$::genta+$atlA_{Efm}$, and *E. faecium* E980 grown in BHI until an OD_{660} of 0.3 or stationary phase by flow cytometry as described previously (47). α-$AtlA_{Efm}$ and α-Acm rabbit immune serum (1:100) was used to detect $AtlA_{Efm}$ and Acm.

$AtlA_{Efm}$, Acm, and eDNA localization. $AtlA_{Efm}$, Acm, and eDNA localization in *E. faecium* was performed on single cells and in the semistatic biofilm model. For single cells, 5 μl of bacteria grown to an OD_{660} of 0.3 or in overnight culture was placed on a coverslip coated with poly-L-lysine and dried at 55°C for 20 min. For both conditions, cells were washed with 3 ml PBS, fixed with 3% paraformaldehyde for 15 min, and washed again with PBS. To identify $AtlA_{Efm}$, Acm, and eDNA, cells were incubated with α-$AtlA_{Efm}$ or α-Acm IgG antibody (1:500 in PBS with 1% bovine serum albumin [BSA]) or monoclonal α-dsDNA (Abcam, Cambridge, MA) (1:1,000 in PBS with 1% BSA) for 1 h on ice and subsequently washed with PBS. A secondary IgG Alexa Fluor 488 goat α-rabbit or α-mouse antibody (Life Technology) (1:500 in PBS with 1% BSA) was added and incubated for an additional 1 h on ice to detect binding to first antibodies. Cells were washed once more and incubated with 5 μg/ml FM 5-95 dye (Invitrogen) for 2 min on ice. Fluorescence was analyzed in the confocal microscope (Leica SP5). Alexa 488 and FM 5-95 were excited at 488 nm. As a control, bacteria were treated as described above but omitting the first antibodies (α-$AtlA_{Efm}$, α-Acm, and α-dsDNA).

eDNA localization in the $AtlA_{Efm}$-deficient mutant by transmission immunoelectron microscopy. Transmission immunoelectron microscopy was performed as described previously with some modifications (50). eDNA in $atlA_{Efm}$::genta overnight culture was labeled with 1:50-diluted specific monoclonal α-dsDNA mouse immune serum (Abcam, Cambridge, MA) in PBS containing 1% bovine serum albumin. For the negative control, this primary antibody step was omitted. Grids were examined using a FEI Tecnai T20 transmission electron microscope at a magnification of ×30,000 to ×65,000, and images were recorded using a digital 4k-by-4k charge-coupled device (CCD) camera.

Effect of $AtlA_{Efm}$ and DNase on *E. faecium* strains. The effect of $AtlA_{Efm}$ and DNase on the phenotype of the E1162 wild type, $atlA_{Efm}$::genta, and $atlA_{Efm}$::genta+$atlA_{Efm}$ was analyzed during bacterial growth under a confocal microscope. The wild type, $atlA_{Efm}$::genta, and $atlA_{Efm}$::genta+$atlA_{Efm}$ were grown in BHI at 37°C for 24 h. After overnight growth, cells were diluted to an OD_{660} of 0.005 in BHI and inoculated with and without purified $AtlA_{Efm}$ (5 μg) or DNase (1.5 μg/μl) in a Lab-Tek chambered eight-well coverglass (Thermo, Fisher Scientific). Cell growth was recorded at regular intervals of 3 min (×40 objective) with the DFC360 FX digital camera kit SP5 (Leica).

ELISA. Binding of the E1162 wild type, $atlA_{Efm}$::genta, and $atlA_{Efm}$::genta+$atlA_{Efm}$ to immobilized fibrinogen, fibronectin, collagen type I, collagen type III, and collagen type IV was assayed by a whole-cell ELISA as described previously (51).

SUPPLEMENTAL MATERIAL

Supplemental material for this article may be found at http://mbio.asm.org/lookup/suppl/doi:10.1128/mBio.00154-13/-/DCSupplemental.

Movie S1, AVI file, 11.6 MB.
Figure S1, TIF file, 0.8 MB.
Figure S2, TIF file, 0.1 MB.
Figure S3, TIF file, 8.9 MB.
Figure S4, TIF file, 0.1 MB.
Figure S5, TIF file, 0.8 MB.
Figure S6, TIF file, 0.1 MB.
Table S1, DOC file, 0.1 MB.
Table S2, DOC file, 0.1 MB.
Table S3, DOC file, 0.1 MB.

ACKNOWLEDGMENTS

Part of this work was supported by ZonMW VENI grant 91610058 to H.L.L. from the Netherlands Organization for Health Research and Development; by a personal Research Grant from the European Society of Clinical Microbiology and Infectious Diseases–ESCMID (2011) to H.L.L.; and by the European Union Seventh Framework Programme (FP7-HEALTH-2011-single-stage) under grant agreement no. 282004, EvoTAR, to R.J.L.W.

REFERENCES

1. **Hidron AI, Edwards JR, Patel J, Horan TC, Sievert DM, Pollock DA, Fridkin SK, National Healthcare Safety Network Team,** Participating National Healthcare Safety Network Facilities. 2008. NHSN annual update: antimicrobial-resistant pathogens associated with healthcare-associated infections: annual summary of data reported to the national healthcare safety network at the Centers for Disease Control and Prevention, 2006–2007. Infect. Control Hosp. Epidemiol. 29:996–1011.
2. **Donlan RM, Costerton JW.** 2002. Biofilms: survival mechanisms of clinically relevant microorganisms. Clin. Microbiol. Rev. **15**:167–193.
3. **Sandoe JA, Witherden IR, Cove JH, Heritage J, Wilcox MH.** 2003. Correlation between enterococcal biofilm formation *in vitro* and medical-device-related infection potential *in vivo*. J. Med. Microbiol. **52**:547–550.
4. **O'Toole G, Kaplan HB, Kolter R.** 2000. Biofilm formation as microbial development. Annu. Rev. Microbiol. **54**:49–79.
5. **Abee T, Kovács AT, Kuipers OP, van der Veen S.** 2011. Biofilm formation and dispersal in Gram-positive bacteria. Curr. Opin. Biotechnol. **22**:172–179.
6. **Allesen-Holm M, Barken KB, Yang L, Klausen M, Webb JS, Kjelleberg S, Molin S, Givskov M, Tolker-Nielsen T.** 2006. A characterization of DNA release in Pseudomonas aeruginosa cultures and biofilms. Mol. Microbiol. **59**:1114–1128.
7. **Petersen FC, Tao L, Scheie AA.** 2005. DNA binding-uptake system: a link between cell-to-cell communication and biofilm formation. J. Bacteriol. **187**:4392–4400.
8. **Ahn SJ, Burne RA.** 2006. The *atlA* operon of *Streptococcus mutans*: role in autolysin maturation and cell surface biogenesis. J. Bacteriol. **188**:6877–6888.
9. **Qin Z, Ou Y, Yang L, Zhu Y, Tolker-Nielsen T, Molin S, Qu D.** 2007. Role of autolysin-mediated DNA release in biofilm formation of Staphylococcus epidermidis. Microbiology **153**:2083–2092.
10. **Vilain S, Pretorius JM, Theron J, Brözel VS.** 2009. DNA as an adhesin: *Bacillus cereus* requires extracellular DNA to form biofilms. Appl. Environ. Microbiol. **75**:2861–2868.
11. **Thomas VC, Hiromasa Y, Harms N, Thurlow L, Tomich J, Hancock LE.** 2009. A fratricidal mechanism is responsible for eDNA release and contributes to biofilm development of *Enterococcus faecalis*. Mol. Microbiol. **72**:1022–1036.
12. **Izano EA, Amarante MA, Kher WB, Kaplan JB.** 2008. Differential roles of poly-*N*-acetylglucosamine surface polysaccharide and extracellular DNA in *Staphylococcus aureus* and *Staphylococcus epidermidis* biofilms. Appl. Environ. Microbiol. **74**:470–476.
13. **Bose JL, Lehman MK, Fey PD, Bayles KW.** 2012. Contribution of the Staphylococcus aureus Atl AM and GL murein hydrolase activities in cell division, autolysis, and biofilm formation. PLoS One **7**:e42244.
14. **Thomas VC, Thurlow LR, Boyle D, Hancock LE.** 2008. Regulation of autolysis-dependent extracellular DNA release by *Enterococcus faecalis* extracellular proteases influences biofilm development. J. Bacteriol. **190**:5690–5698.
15. **Heilmann C, Hartleib J, Hussain MS, Peters G.** 2005. The multifunctional *Staphylococcus aureus* autolysin Aaa mediates adherence to immobilized fibrinogen and fibronectin. Infect. Immun. **73**:4793–4802.
16. **Allignet J, Aubert S, Dyke KG, El Solh N.** 2001. Staphylococcus caprae strains carry determinants known to be involved in pathogenicity: a gene encoding an autolysin-binding fibronectin and the *ica* operon involved in biofilm formation. Infect. Immun. **69**:712–718.
17. **Heilmann C, Hussain M, Peters G, Götz F.** 1997. Evidence for autolysin-mediated primary attachment of Staphylococcus epidermidis to a polystyrene surface. Mol. Microbiol. **24**:1013–1024.
18. **Liu G, Xiang H, Tang X, Zhang K, Wu X, Wang X, Guo N, Feng H, Wang G, Liu L, Shi Q, Shen F, Xing M, Yuan P, Liu M, Yu L.** 2011. Transcriptional and functional analysis shows sodium houttuyfonate-

mediated inhibition of autolysis in Staphylococcus aureus. Molecules **16**: 8848–8865.
19. **Schlag M, Biswas R, Krismer B, Kohler T, Zoll S, Yu W, Schwarz H, Peschel A, Götz F.** 2010. Role of staphylococcal wall teichoic acid in targeting the major autolysin Atl. Mol. Microbiol. **75**:864–873.
20. **O'Gara JP.** 2007. ica and beyond: biofilm mechanisms and regulation in Staphylococcus epidermidis and Staphylococcus aureus. FEMS Microbiol. Lett. **270**:179–188.
21. **Nallapareddy SR, Weinstock GM, Murray BE.** 2003. Clinical isolates of *Enterococcus faecium* exhibit strain-specific collagen binding mediated by ACM, a new member of the MSCRAMM family. Mol. Microbiol. **47**: 1733–1747.
22. **Shockman GD, Holtje J-V.** 1994. Microbial peptidoglycan (murein) hydrolases, p 131–166. **In** Ghuysen J-M, Hakenbeck R (ed), Bacterial cell wall. Elsevier, Amsterdam, the Netherlands.
23. **Eckert C, Lecerf M, Dubost L, Arthur M, Mesnage S.** 2006. Functional analysis of AtlA, the major *N*-acetylglucosaminidase of *Enterococcus faecalis*. J. Bacteriol. **188**:8513–8519.
24. **Buist G, Steen A, Kok J, Kuipers OP.** 2008. LysM, a widely distributed protein motif for binding to (peptido)glycans. Mol. Microbiol. **68**: 838–847.
25. **Marchler-Bauer A, Zheng C, Chitsaz F, Derbyshire MK, Geer LY, Geer RC, Gonzales NR, Gwadz M, Hurwitz DI, Lanczycki CJ, Lu F, Lu S, Marchler GH, Song JS, Thanki N, Yamashita RA, Zhang D, Bryant SH.** 2013. CDD: conserved domains and protein three-dimensional structure. Nucleic Acids Res. **41**:D348–D352.
26. **Emirian A, Fromentin S, Eckert C, Chau F, Dubost L, Delepierre M, Gutmann L, Arthur M, Mesnage S.** 2009. Impact of peptidoglycan O-acetylation on autolytic activities of the *Enterococcus faecalis* N-acetylglucosaminidase AtlA and N-acetylmuramidase AtlB. FEBS Lett. **583**:3033–3038.
27. **Shibata Y, Kawada M, Nakano Y, Toyoshima K, Yamashita Y.** 2005. Identification and characterization of an autolysin-encoding gene of *Streptococcus mutans*. Infect. Immun. **73**:3512–3520.
28. **Mohamed JA, Huang W, Nallapareddy SR, Teng F, Murray BE.** 2004. Influence of origin of isolates, especially endocarditis isolates, and various genes on biofilm formation by *Enterococcus faecalis*. Infect. Immun. **72**: 3658–3663.
29. **Gross M, Cramton SE, Götz F, Peschel A.** 2001. Key role of teichoic acid net charge in *Staphylococcus aureus* colonization of artificial surfaces. Infect. Immun. **69**:3423–3426.
30. **Koprivnjak T, Mlakar V, Swanson L, Fournier B, Peschel A, Weiss JP.** 2006. Cation-induced transcriptional regulation of the *dlt* operon of *Staphylococcus aureus*. J. Bacteriol. **188**:3622–3630.
31. **Mesnage S, Chau F, Dubost L, Arthur M.** 2008. Role of N-acetylglucosaminidase and N-acetylmuramidase activities in *Enterococcus faecalis* peptidoglycan metabolism. J. Biol. Chem. **283**:19845–19853.
32. **Barnes AM, Ballering KS, Leibman RS, Wells CL, Dunny GM.** 2012. Enterococcus faecalis produces abundant extracellular structures containing DNA in the absence of cell lysis during early biofilm formation. mBio **3**(4):e00193-12.
33. **Li YH, Lau PC, Tang N, Svensäter G, Ellen RP, Cvitkovitch DG.** 2002. Novel two-component regulatory system involved in biofilm formation and acid resistance in *Streptococcus mutans*. J. Bacteriol. **184**:6333–6342.
34. **Li YH, Tang N, Aspiras MB, Lau PC, Lee JH, Ellen RP, Cvitkovitch DG.** 2002. A quorum-sensing signaling system essential for genetic competence in *Streptococcus mutans* is involved in biofilm formation. J. Bacteriol. **184**:2699–2708.
35. **Wen ZT, Burne RA.** 2002. Functional genomics approach to identifying genes required for biofilm development by *Streptococcus mutans*. Appl. Environ. Microbiol. **68**:1196–1203.
36. **Koraimann G.** 2003. Lytic transglycosylases in macromolecular transport systems of gram-negative bacteria. Cell. Mol. Life Sci. **60**:2371–2388.
37. **Miller EJ, Gay S.** 1987. The collagens: an overview and update. Methods Enzymol. **144**:3–41.
38. **Qin X, Singh KV, Xu Y, Weinstock GM, Murray BE.** 1998. Effect of disruption of a gene encoding an autolysin of *Enterococcus faecalis* OG1RF. Antimicrob. Agents Chemother. **42**:2883–2888.
39. **Paganelli FL, Willems RJ, Leavis HL.** 2012. Optimizing future treatment of enterococcal infections: attacking the biofilm? Trends Microbiol. **20**: 40–49.
40. **van Schaik W, Top J, Riley DR, Boekhorst J, Vrijenhoek JE, Schapendonk CM, Hendrickx AP, Nijman IJ, Bonten MJ, Tettelin H, Willems RJ.** 2010. Pyrosequencing-based comparative genome analysis of the nosocomial pathogen *Enterococcus faecium* and identification of a large transferable pathogenicity island. BMC Genomics **11**:239.
41. **Leenhouts K, Buist G, Bolhuis A, ten Berge A, Kiel J, Mierau I, Dabrowska M, Venema G, Kok J.** 1996. A general system for generating unlabelled gene replacements in bacterial chromosomes. Mol. Gen. Genet. **253**:217–224.
42. **Zhang X, Paganelli FL, Bierschenk D, Kuipers A, Bonten MJ, Willems RJ, van Schaik W.** 2012. Genome-wide identification of ampicillin resistance determinants in *Enterococcus faecium*. PLoS Genet. **8**:e1002804.
43. **Zhang X, Vrijenhoek JE, Bonten MJ, Willems RJ, van Schaik W.** 2011. A genetic element present on megaplasmids allows *Enterococcus faecium* to use raffinose as carbon source. Environ. Microbiol. **13**:518–528.
44. **Chaudhuri RR, Allen AG, Owen PJ, Shalom G, Stone K, Harrison M, Burgis TA, Lockyer M, Garcia-Lara J, Foster SJ, Pleasance SJ, Peters SE, Maskell DJ, Charles IG.** 2009. Comprehensive identification of essential Staphylococcus aureus genes using transposon-mediated differential hybridisation (TMDH). BMC Genomics **10**:291.
45. **Liu Y, Burne RA.** 2011. The major autolysin of *Streptococcus gordonii* is subject to complex regulation and modulates stress tolerance, biofilm formation, and extracellular-DNA release. J. Bacteriol. **193**:2826–2837.
46. **Ju CX, Gu HW, Lu CP.** 2012. Characterization and functional analysis of *atl*, a novel gene encoding autolysin in *Streptococcus suis*. J. Bacteriol. **194**: 1464–1473.
47. **Heikens E, Bonten MJ, Willems RJ.** 2007. Enterococcal surface protein Esp is important for biofilm formation of *Enterococcus faecium* E1162. J. Bacteriol. **189**:8233–8240.
48. **Heydorn A, Nielsen AT, Hentzer M, Sternberg C, Givskov M, Ersbøll BK, Molin S.** 2000. Quantification of biofilm structures by the novel computer program COMSTAT. Microbiology **146**:2395–2407.
49. **Bardoel BW, van Kessel KP, van Strijp JA, Milder FJ.** 2012. Inhibition of Pseudomonas aeruginosa virulence: characterization of the AprA-Apri interface and species selectivity. J. Mol. Biol. **415**:573–583.
50. **Hendrickx AP, van Wamel WJ, Posthuma G, Bonten MJ, Willems RJ.** 2007. Five genes encoding surface-exposed LPXTG proteins are enriched in hospital-adapted *Enterococcus faecium* clonal complex 17 isolates. J. Bacteriol. **189**:8321–8332.
51. **Hendrickx AP, van Luit-Asbroek M, Schapendonk CM, van Wamel WJ, Braat JC, Wijnands LM, Bonten MJ, Willems RJ.** 2009. SgrA, a nidogen-binding LPXTG surface adhesin implicated in biofilm formation, and EcbA, a collagen binding MSCRAMM, are two novel adhesins of hospital-acquired *Enterococcus faecium*. Infect. Immun. **77**:5097–5106.